Effect of anatomical differences and intraocular lens design on negative dysphotopsia

Vught, L. van; Que, I.; Luyten, G.P.M.; Beenakker, J.W.M.

Open

LABORATORY SCIENCE

Effect of anatomical differences and intraocular lens design on negative dysphotopsia

Luc van Vught, BSc, Ivo Que, Gregorius P.M. Luyten, MD, PhD, FEBOphth, Jan-Willem M. Beenakker, MSc, PhD

Purpose: To assess the effect of ocular anatomy and intraocular lens (IOL) design on negative dysphotopsia (ND).

Setting: Department of Ophthalmology, Leiden University Medical Center, Leiden, the Netherlands.

Design: Ray-tracing study based on clinical data.

Methods: Ray-tracing simulations were performed to assess the effect of anatomical differences and differences in IOL design on the peripheral retinal illumination. To that end, eye models that incorporate clinically measured anatomical differences between eyes of patients with ND and eyes of pseudophakic controls were created. The anatomical differences included pupil size, pupil centration, and iris tilt. The simulations were performed with different IOL designs, including a simple biconvex IOL design and a more complex clinical IOL design with a convex–concave anterior surface. Both IOL designs were analyzed using a clear edge and a frosted edge. As ND is generally considered to be caused by a discontinuity in peripheral retinal illumination, this illumination profile was determined for each eye model and the severity of the discontinuity was compared between eye models.

Results: The peripheral retinal illumination consistently showed a more severe discontinuity in illumination with ND-specific anatomy. This difference was the least pronounced, 8%, with the frosted edge clinical IOL and the most pronounced, 18%, with the clear edge biconvex IOL.

Conclusions: These results show that small differences in the ocular anatomy or IOL design affect the peripheral retinal illumination. Therewith, they can increase the severity of ND by up to 18%.

J Cataract Refract Surg 2022; 48:1446–1452 Copyright © 2022 The Author(s). Published by Wolters Kluwer Health, Inc. on behalf of ASCRS and ESCRS

Negative dysphotopsia (ND) is a relatively common complaint after cataract surgery or refractive lens exchange with intraocular lens (IOL) implantation, often described as a shadow or missing area in the temporal peripheral visual field (VF).[1–3] The incidence is reported to be up to 19% when actively evaluated during clinical follow-up, but fortunately in most cases, it resolves over time.[4,5] However, complaints remain present in approximately 3% of the patients with little chance on further improvement.[5] The severity of the remaining shadow differs between patients, leaving some patients with mild VF defects, whereas others experience bothersome complaints that disturb their daily life.[3,6]

Clinical studies have identified multiple factors that potentially contribute to ND, including a smaller pupil size, a tilted anterior chamber geometry, a larger overlap of the anterior capsule, an increased angle kappa, a noninferotemporal orientation of the optic–haptic junction of the IOL, and a smaller IOL diameter.[3,6–11] Although ND can occur with different types of in-the-bag implanted IOLs, it has not been reported with anterior chamber IOLs or sulcus-fixated IOLs.[8] One of the major problems in the clinical evaluation of ND is the lack of methods to objectively quantify this far-peripheral visual complaint. Thus far, only Goldmann perimetry has been able to show the loss of peripheral vision in some, but not all, eyes.[12]

To overcome this lack of objective measurements and to obtain additional insight, multiple ray-tracing studies of ND have been performed. Within these studies, the path of light through the eye is calculated. Based on these studies, it is proposed that ND is caused by a gap in the illumination of the nasal retina, which is then experienced as a shadow in the temporal VF.[2,13–15] These simulations

Submitted: May 23, 2022 | Final revision submitted: August 30, 2022 | Accepted: August 30, 2022

From the Department of Ophthalmology, Leiden University Medical Center, Leiden, the Netherlands (van Vught, Luyten, Beenakker); C.J. Gorter Center for High Field MRI, Department of Radiology, Leiden University Medical Center, Leiden, the Netherlands (van Vught, Beenakker); Translational Nanobiomaterials and Imaging Group, Department of Radiology, Leiden University Medical Center, Leiden, the Netherlands (Que); Department of Radiation Oncology, Leiden University Medical Center, Leiden, the Netherlands (Beenakker).

This study was supported by the ESCRS (Co Dublin, Ireland) and Stichting Leids Oogheelkundig Ondersteuningsfonds (Oegstgeest, the Netherlands).

Corresponding author: Luc van Vught, BSc, Department of Ophthalmology, Leiden University Medical Center, Albinusdreef 2, 2333 ZA Leiden, the Netherlands. Email: L.van_vught@lumc.nl.

0886-3350/$ - see frontmatter
https://doi.org/10.1097/j.jcrs.0000000000001054

showed that this gap is the result of a discontinuity between light passing between the iris and the IOL (the iris–IOL gap) and light refracted by the IOL. Many factors that potentially affect this gap have been proposed through these simulations, including a larger angle kappa, a smaller pupil diameter, the axial distance between the IOL and the iris, the refractive index, the diameter of the IOL, and the shape of the IOL.[13,16,17]

Although these ray-tracing simulations have provided valuable insights in potential causes of ND, they used generic eye models that do not fully reflect the anatomy of eyes with ND. Recently, we presented clinical data of a cohort of pseudophakic eyes with and without ND, showing that eyes with ND have a smaller and more temporally decentered pupil and a larger temporal tilt of the iris (Figure 1).[7] Furthermore, we showed that the anterior chamber distance, the distance between the iris and the IOL, and the peripheral retinal shape were comparable between both groups.[7,18] Within this study, we aim to assess the optical consequences of the anatomical differences observed in the ND population and the effect of different IOL designs on the peripheral illumination, in particular related to the temporal shadow that is perceived by patients with ND.

METHODS

To accurately assess the relation between anatomical properties of the eye and the occurrence of ND, ray-tracing simulations were performed using eye models that closely reflect the actual ocular anatomy of eyes with and without ND. Based on the reported clinical differences between eyes with and without ND, 2 eye models were designed, 1 with a typical anatomy for patients with ND and 1 with a typical anatomy for pseudophakic controls (Figure 1).[7,18] The anatomical aspects of these eye models were derived from clinical measurements obtained from 37 patients with ND and 26 pseudophakic controls who participated in the ESCRS vRESPOND study (CCMO registry number: NL58358.058.16). Before participation, all subjects provided written informed consent. The study was performed in conformance with the tenets of the Declaration of Helsinki and was approved by the local Medical Ethics Committee.

Model Design

Simulations were performed in OpticStudio (v. 20.3.2, Zemax, LCC) using a highly modified version of the Escudero-Sanz eye model and a 543 nm light source (Figure 1).[19] The entire process of constructing eye models and performing the nonsequential ray-tracing simulations was fully automated through the OpticStudio API and Python (v. 3.7) using the open source ZOSPy package.[20] The resulting ND eye model and control eye model, both with a biconvex IOL, are available in the supplementary information (Supplemental Data available at https://github.com/MREYE-LUMC/ZOSPy/tree/main/examples).

To correspond to the clinical measurements and to reflect the subject's perception, the eye models were constructed relative to the visual axis, instead of the more commonly used, but clinically less relevant, optical axis. The anatomical properties of the eye that have shown to be significantly different between patients with ND and pseudophakic controls, including iris tilt, pupil centration and pupil diameter, were adjusted in each model (Figure 1, B).[7] All other anatomical properties were based on either the average of both groups combined or the values reported by Escudero-Sanz et al. (Figure 1, A).[7,18,19]

As the average corneal shape did not differ significantly between patients with ND and pseudophakic controls, the corneal shape of the Escudero-Sanz eye model eye was used.[7,19] The anterior corneal surface was modeled as an ellipsoidal surface with a radius of 7.72 mm and a conic constant of −0.26, while for its posterior surface, a radius of 6.50 mm without conic component was used.[19] The central thickness of the cornea was 0.55 mm, and its refractive index was modeled as 1.3777.[19] The refractive indices of the anterior chamber and vitreous body were defined as 1.3391 and 1.3377, respectively.[19]

As the anterior chamber depth and iris–IOL distance were found to be similar in patients with ND and pseudophakic controls, a common distance of 3.12 mm between the posterior corneal surface and the anterior iris surface was used for both groups.[7,18] Furthermore, the iris thickness was 0.55 mm, and the pupil edges were sloping inward toward the center.[21,22] To match the clinically measured differences in iris orientation and pupil location and size, the iris was tilted temporally by 6.5 degrees in the ND model and 4.0 degrees in the control model. Furthermore, the pupil diameter was defined as 2.4 mm in the ND model and 3.0 mm in the control model. Finally, the pupil center of the ND model was moved 0.17 mm temporally about the visual axis, while the pupil center of the control model was shifted 0.01 mm nasally.[7]

As ND has been reported to occur with a wide variety of posterior chamber IOL designs, each eye model was analyzed with 4 different IOL designs (Figure 1, C).[7,8] The first design consisted of a simple biconvex IOL design, similar to those used in earlier ray-tracing studies.[2,13,16] In reality, however, IOLs often have a more complex design.[23] Therefore, the second design matched the convex–concave anterior surface and convex posterior surface of the ZCB00 IOL (Johnson & Johnson Vision), as obtained through μCT scanning (Supplemental Figure 1, http://links.lww.com/JRS/A704).[24] Clinically, the shape of the edge differs between IOLs, and some IOLs have a frosted edge that is intended to scatter incident rays.[24–27] Unfortunately, the optical characteristics, including the edge shape and scattering properties, are not available for most IOLs. As the μCT images showed the edge of the clinical IOL to be straight, this was used a reference to model the edges of both IOLs. In addition, the ray-tracing study by Franchini et al. suggests the maximum scattering of a frosted IOL edge to be 17.5%.[28] To assess the effect of a frosted edge, the edge of each IOL was thus modeled as both a 0% and a 17.5% Lambertian scattering surface (Figure 1, C). All IOLs had a refractive index of 1.47, and the distance between the posterior iris surface and the IOL was 0.57 mm for all IOLs.[18] The IOLs were positioned parallel to the (tilted) iris and centered on the pupil center.[18]

As the peripheral retinal shape did not significantly differ between patients with ND and controls, a common ellipsoid model was used to describe the retina, with a horizontal and vertical radius of 11.75 mm and a central radius of 10.55 mm (Figure 1, A).[18,29] The axial length of both models was 23.81 mm, reflecting the average of the study population.[18]

Peripheral Retinal Illumination

The peripheral retinal illumination was assessed using a 4.0 mm wide circular light source that emitted 10^5 parallel rays of light. This source rotated from VF angles (VFAs) of −10 degrees nasally to 120 degrees temporally in 0.25-degree steps. The retinal surface consisted of detectors with a resolution of 0.1 degree horizontally by 0.1 mm vertically. The location of each detector was expressed as its angle about the visual axis and retinal center. Similar to the study of Simpson, a separate set of simulations was performed to relate the location of each detector to the VFA experienced by the subject (Supplemental Figure 2, http://links.lww.com/JRS/A705).[22] The illumination profiles of all VF input angles were summed to obtain the total retinal illumination profile (Figure 2). As pupil diameters differ between models, all results were normalized to the total illumination perceived at 50 degrees temporally in the VF.

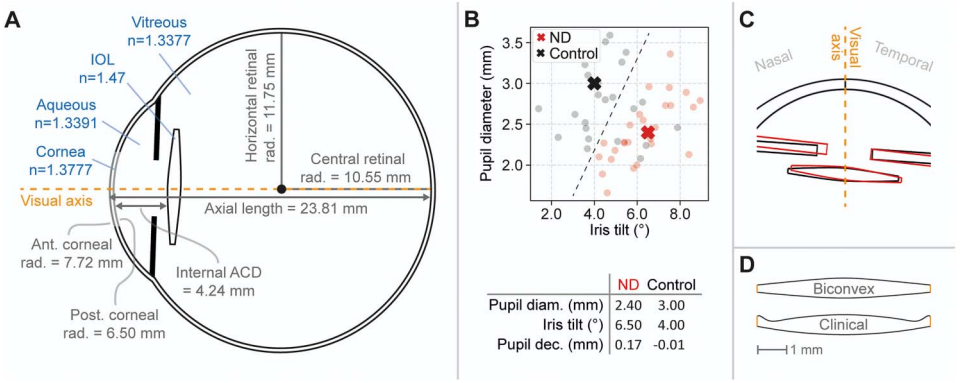

Figure 1. Eye model specifications. *A*: Schematic view of the eye model including principal model specifications. *B*: Anterior chamber geometry of patients with ND (*red*) and pseudophakic controls (*black*). Actual values used for the eye models are given in the table and annotated in the plot using crosses. *C*: Detailed overview of the anterior chamber anatomy of patients with ND (*red*) and pseudophakic controls (*black*). *D*: Schematic view of the biconvex (*upper*) and clinical (*lower*) IOL model. The edge of the IOL (*orange*) was defined as either a clear edge or an edge with Lambertian scattering. ND = negative dysphotopsia

To determine which image features corresponded to rays passing through the iris–IOL gap or through the IOL edge, separate simulations were performed in which these specific rays were isolated from the other rays (Figure 2, B).

Quantification

Three aspects of the peripheral retinal illumination were quantified (Figure 2, C). First, the start of the retinal illumination gap, defined as the VFA with a relative retinal illumination below 0.2, was determined. In addition, the maximum intensity of the rays passing through the iris–IOL gap was determined, together with the corresponding VFA. Finally, the severity of the retinal illumination gap, defined as the total reduction in relative illumination compared with the maximum intensity of the rays passing through the iris–IOL gap, was calculated.

RESULTS

All eye models were successfully simulated and analyzed. An example of a resulting eye model is shown in Figure 2, A. The central spherical equivalent of refraction of the eye models ranged from −1.2 to +0.5 diopters. All models showed an approximately equal relation between retinal angle and perceived VFA. The same relation was therefore used for all models, approximated by a second order polynomial: $\alpha_{VF} = \frac{1.1 \times 10^{-3}}{\text{degree}}\alpha_R^2 - 0.60\alpha_R + 0.17\,\text{degree}$, with α_{VF} being the apparent VFA and α_R being the retinal angle, both in degrees (Supplemental Figure 2, http://links.lww.com/JRS/A705).

In all eye models, the simulations showed a similar gradually decreasing illumination toward peripheral vision. At a VFA of 50 degrees, the angle used as a normalization reference for subsequent evaluations and the control model received a 1.5 times higher illumination than the ND model, reflecting the smaller pupil size in the ND population. The reference illumination did not differ between the studied IOLs. A strong decrease in illumination was observed starting at approximately 80 degrees, which was partially caused by rays passing through the IOL edge instead of through the posterior IOL surface and partially by vignetting of the iris. The profile of this decrease and the VFA at which it occurred depended strongly on IOL design. An area of low illumination, the retinal illumination gap, was observed. This area was followed by a local increase in illumination that was the result of rays passing through the iris–IOL gap. A complete overview of the contribution of rays passing through specific intraocular structures is provided in Figure 4 and summarized in Figure 2, B.

Differences in peripheral retinal illumination were clearly visible between IOL designs and were predominantly induced by rays passing through the IOL edge (Figures 3 and 4). For the biconvex IOL with a clear edge, the relative illumination decreased below 0.2 between VFAs of 85 degrees and 90 degrees and rays passing through the edge induced a local increase in illumination at a VFA of approximately 75 degrees

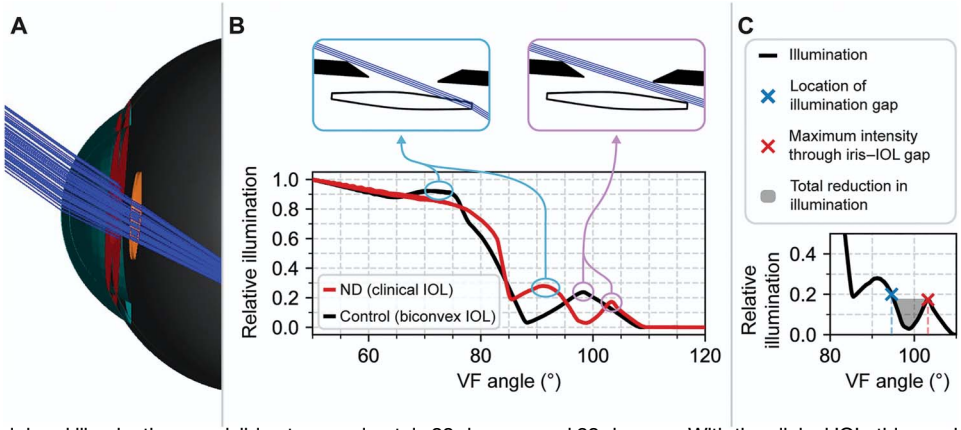

Figure 2. Examples of the total retinal illumination profile. *A*: Example of a 3D eye model illuminated by a peripheral beam of light. *B*: Breakdown of the total peripheral retinal illumination as a function of the VF angle for the ND model with a clinical IOL (*red*) and the control model with biconvex clinical IOL (*black*). The contributions of rays passing through the IOL edge (*light blue circles*, *left insert*) and those passing through the iris–IOL gap (*light purple circles*, *right insert*) show distinct differences between IOL designs. Discontinuities in peripheral illumination are visible at approximately 88 degrees and 98 degrees. With the clinical IOL, this gap is partially filled by rays passing through the IOL edge. *C*: Example of quantification of the discontinuity in peripheral retinal illumination. ND = negative dysphotopsia; VF = visual field

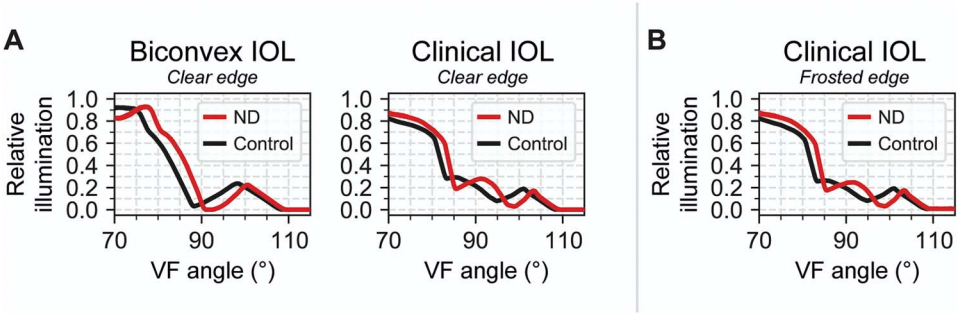

Figure 3. Peripheral retinal illumination. Normalized retinal illumination profiles for the ND model (*red*) and the control model (*black*). *A*: Illumination with a clear edge design. Clear differences between the biconvex and the clinical IOL are visible, primarily caused an increase in illumination at a VF angle of approximately 90 degrees with the clinical IOL. This increase is attributed to rays passing through the IOL edge that partially fill the illumination gap (Figure 4). *B*: The illumination profile of a clinical IOL with a frosted edge design shows slight differences in the maximum intensity around a VF angle of 90 degrees because the rays through the edge of the IOL are partially dispersed by the frosted edge. Data for the biconvex IOL with a frosted edge showed a similar profile compared with the clear edge design and are shown in Figure 4. ND = negative dysphotopsia; VF = visual field

(Table 1 and Figure 3). For the clinical IOL design, however, the relative illumination decreased below 0.2 between 90 degrees and 95 degrees and the local increase in illumination caused by rays passing through the edge was observed at approximately 90 degrees (Table 1). In addition, part of these rays illuminated the illumination gap, resulting in a lower depth of the shadow (Figure 3). With a frosted IOL edge, the rays were dispersed over the peripheral retina for both IOL designs. This dispersion had an insignificant effect on the peripheral illumination profile of the biconvex IOL design and a small effect on the peripheral illumination profile of the clinical IOL design, reducing the VFA at which the relative illumination decreased below 0.2 by approximately 1 degree (Table 1 and Figure 3).

The far peripheral illumination, caused by light passing through the iris–IOL gap, differed between IOL designs. Overall, the VFA at which light started passing through this gap was approximately 2 degrees lower in the control models. In addition, approximately 1.9 times more light rays passed through the iris–IOL gap in simulations with the biconvex IOL model than in simulations with the clinical IOL model. Furthermore, the number of light rays passing through the iris–IOL gap was 2.4 times higher with the control models compared with the ND models.

For all IOL designs, a more severe shadow was observed in the ND model. For the biconvex IOL with a clear edge design, the severity was 18% higher in the ND model compared with the control model. A similar increase in shadow severity was observed with the clinical IOL, where

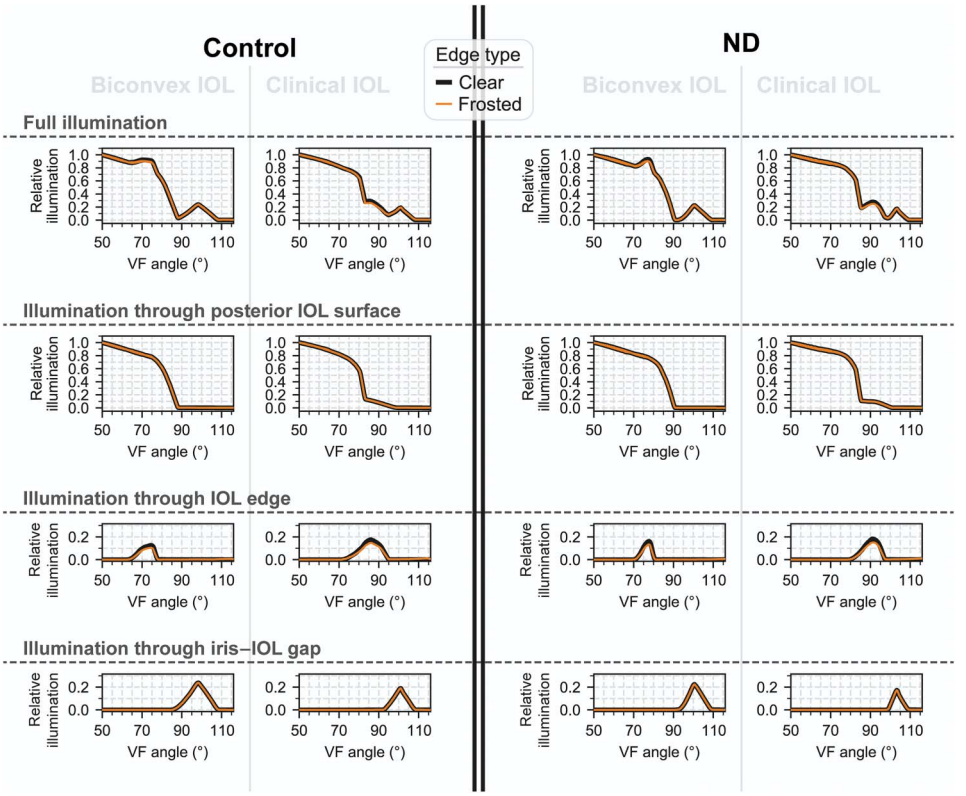

Figure 4. The influence of specific sets of rays on the peripheral illumination profile. Data are shown for the control (*left*) and ND (*right*), as well as for the biconvex IOL (*left column*) and clinical IOL (*right column*), both with a clear edge design (*black*) and a frosted edge design (*cyan*). The complete illumination, illumination by rays through the posterior IOL surface, illumination by rays through the IOL edge, and illumination by rays through the iris–IOL gap, is shown. Local increases in illumination can clearly be seen for rays passing through the IOL edge and rays passing through the iris–IOL gap. ND = negative dysphotopsia; VF = visual field

Table 1. Quantification of the peripheral illumination gap.

Parameter	Biconvex IOL Clear edge		Clinical IOL Clear edge		Biconvex IOL Frosted edge		Clinical IOL Frosted edge	
	ND	Control	ND	Control	ND	Control	ND	Control
Location of illumination gap (VFA, °)	89	86	95	91	89	86	94	90
Location of maximal illumination through iris–IOL gap (VFA, °)	101	98	103	101	101	98	103	101
Shadow severity (% difference with control)	18	—	15	—	17	—	8.0	—

ND = negative dysphotopsia; VF = visual field angle

Apparent visual angle at which the illumination decreases below 0.2 and the angle of maximum illumination through the iris–IOL gap are given for all models. Shadow severity in ND is expressed as % difference with the corresponding control model. The models with ND consistently showed a more severe shadow compared with their equivalent control models.

the reduction in illumination was 15% stronger in the ND model. For the biconvex IOL, the simulations with the frosted edge did not differ from those with a clear edge. For the clinical IOL design, however, a frosted edge reduced the shadow severity from 15% to 8% (Table 1 and Figure 3, B).

DISCUSSION

Within this study, we demonstrated that ND-related anatomical differences can decrease the peripheral retinal illumination. In addition, we showed the effects of IOL design on the retinal illumination profile. Combined, they can increase the severity of a shadow-like area on the peripheral retina by an up to 18%. These results strengthen the common assumption that ND is related to an illumination gap of the peripheral retina, as proposed by Holladay and Simpson.[13,15,16] Furthermore, we introduced several new improvements to the conventional ray-tracing methods, which aims to provide a more realistic assessment of the optics in a specific patient population and a better relation between the results and the clinical measurements.

As the results from any simulation study depend strongly on the used model, clinically measured anatomical differences in pupil diameter and iris tilt were incorporated in the eye models. Although some studies have already assessed the effect of specific anatomical variations of a generic eye model, the clinical value of these studies was generally limited because they did not incorporate the ocular anatomy that is specific for patients with ND.[13,16] In addition, more realistic IOL designs were included in the evaluations. However, although the clinical IOL design was based on μCT data of the ZCB00 IOL, the exact design of the IOL was not known. As the study showed a direct relation between IOL edge design and peripheral illumination profile, additional information on the edge curvature and type of frosting could further improve the accuracy of the simulations.[23,28] As the μCT images (Supplemental Figure 1, http://links.lww.com/JRS/A704) do not show any curvature at the IOL edge, a curved edge, such as used for the Clareon CNA0T0 IOL, is not expected.[23] A different scattering profile could, however, strongly affect the peripheral retinal illumination, as shown by additional simulations with a 100% Lambertian scattering edge (Supplemental Figure 3, http://links.lww.com/JRS/A706). Nonetheless, such high scattering coefficients have not been reported for IOLs.[28]

In this study, the visual axis, instead of the more conventional optical axis, was used as a reference axis for the eye model. This allows for a better correlation between simulations, patient's vision, and clinical measurements, as the latter 2 are determined relative to the visual axis.[12] To this end, the relation between retinal location and VFA was determined. Although an extrapolated relation was used for VFAs above 78 degrees, we do not expect this to affect the study results because the scaling proved to be the same for the studied models.

Another difference regarding most earlier ray-tracing studies is the use of nonsequential instead of sequential ray tracing.[15,16,22] In sequential ray tracing, rays of light are assumed to pass through all defined surfaces sequentially. Although this assumption allows for many powerful analyses, such as the determination of the ocular aberration profile, these analyses are erroneous when light rays miss an optical element, which is one of the proposed origins of ND.[7,19,30,31] The use of nonsequential ray tracing can explain the differences between the presented retinal illumination profiles and the profiles of earlier sequential studies, which seem to miss the contribution of light rays passing through the edge of the IOL (Supplemental Figure 2, http://links.lww.com/JRS/A705).[16] However, ray aiming, an OpticStudio feature which assures that the complete pupil is illuminated, is not available for nonsequential ray tracing. This limitation was resolved by using a relatively large input beam diameter of 4.0 mm, which assures the complete illumination of the pupil at high input angles.

This study showed that the incorporation of relevant clinical differences in the eye model has a direct effect on the peripheral vision because it resulted in an up to 18% increase of the peripheral illumination gap and other differences in the peripheral illumination. In the ND eye model with a frosted edge clinical IOL design, for example, the peripheral illumination profile shows a large area of low illumination, in contrast to the smaller area with a total absence of illumination which was observed with the clear edge biconvex IOL used in earlier studies.[16,22] These differences might explain why some patients describe ND as completely missing a part of the temporal VF, while others describe it as a shade.[12]

In the peripheral illumination of the pseudophakic control model, an area of decreased illumination was also observed. Although it is less pronounced than in the

corresponding ND models, this finding was unexpected because these subjects did not report any ND-related complaints. It was furthermore unexpected that the decrease in peripheral illumination was the least pronounced with the frosted edge clinical IOL design because the clinical IOL on which the model was based is reported to cause ND in some patients.[7,24] However, the identified 8% difference might still be sufficient to experience ND, and more research on the relation with the experienced shadow is required, especially since additional simulations with a higher degree of scattering seem to further reduce severity of ND (Supplemental Figure 3, http://links.lww.com/JRS/A706, Supplemental Table 1, http://links.lww.com/JRS/A707).

This unexpected observation might also show the necessity to fully personalize the ray-tracing models, so they can be directly related to the subjects' visual perception. For central vision, such simulations have been proposed.[32] For the far peripheral vision, these simulations are of higher complexity, especially because photoreceptor density and extend of the functional retina likely differ between subjects.[14,33] However, these assessments might contribute to the understanding of why the illumination gap observed in the control population, although less severe, is not perceived as a burdensome temporal shadow.

This study showed the effect of IOL design on the peripheral illumination profile, in particular on the light passing through the iris–IOL gap. These differences might explain why certain surgical interventions, such as IOL exchange with a wide optic IOL or orienting the haptics horizontally on IOL implantation, can resolve ND by interacting with the iris–IOL gap.[10,11,34] However, the analyses presented in this study only evaluated a subset of the possible IOL design choices, which for example also include the refractive index, edge thickness, and position regarding the pupil. Future studies will therefore likely require a detailed modeling of the implanted IOL because these optical effects of all these factors interact with each other, and this study shows that even small changes have a direct impact on the peripheral illumination profile.

Similarly, because small variations in the ocular anatomy of an individual patient can influence the peripheral illumination profile, a one-size-fits-all solution for ND is unlikely and probably requires full personalization of the eye model.[7,30,31,35] An extension of the current analyses, including wide optic IOLs, piggyback IOL implantation, or variation in IOL haptics orientation, might therefore aid to determine which treatment is optimal for a specific ocular anatomy.[10,11,17,36] To that end, the eye models have been made available online (Supplemental Data available at https://github.com/MREYE-LUMC/ZOSPy/tree/main/examples) and the ZOSPy package, used to automate the design and evaluation of the eye models in OpticStudio, has been published open source.[20]

In conclusion, this research demonstrates that clinically observed differences in the ocular anatomy of patients with ND have a strong, up to 18%, effect on the severity of the discontinuation of peripheral retinal illumination. It furthermore demonstrated the impact of the IOL design on this peripheral shadow.

WHAT WAS KNOWN

- Negative dysphotopsia (ND) is proposed to originate from a reduced peripheral retinal illumination caused by light rays passing through the gap between the iris and the IOL.
- The anterior chamber geometry is significantly different between patients with ND and pseudophakic controls.

WHAT THIS PAPER ADDS

- The anatomical differences between patients with ND and pseudophakic controls affect the illumination of the peripheral retina.
- There is an evident relation between ocular anatomy, IOL design, and the resulting peripheral retinal illumination.

REFERENCES

1. Davison JA. Positive and negative dysphotopsia in patients with acrylic intraocular lenses. J Cataract Refract Surg 2000;26:1346–1355
2. Holladay JT, Zhao H, Reisin CR. Negative dysphotopsia: the enigmatic penumbra. J Cataract Refract Surg 2012;38:1251–1265
3. Masket S, Fram NR. Pseudophakic dysphotopsia: review of incidence, cause, and treatment of positive and negative dysphotopsia. Ophthalmology 2021;128:e195–e205
4. Makhotkina NY, Nijkamp MD, Berendschot T, van den Borne B, Nuijts R. Effect of active evaluation on the detection of negative dysphotopsia after sequential cataract surgery: discrepancy between incidences of unsolicited and solicited complaints. Acta Ophthalmol 2018;96:81–87
5. Osher RH. Negative dysphotopsia: long-term study and possible explanation for transient symptoms. J Cataract Refract Surg 2008;34:1699–1707
6. Henderson BA, Geneva II. Negative dysphotopsia: a perfect storm. J Cataract Refract Surg 2015;41:2291–2312
7. van Vught L, Luyten GPM, Beenakker JM. Distinct differences in anterior chamber configuration and peripheral aberrations in negative dysphotopsia. J Cataract Refract Surg 2020;46:1007–1015
8. Masket S, Fram NR. Pseudophakic negative dysphotopsia: surgical management and new theory of etiology. J Cataract Refract Surg 2011;37:1199–1207
9. Folden DV. Neodymium:YAG laser anterior capsulectomy: surgical option in the management of negative dysphotopsia. J Cataract Refract Surg 2013;39:1110–1115
10. Henderson BA, Yi DH, Constantine JB, Geneva II. New preventative approach for negative dysphotopsia. J Cataract Refract Surg 2016;42:1449–1455
11. Bonsemeyer MK, Becker E, Liekfeld A. Dysphotopsia and functional quality of vision after implantation of an intraocular lens with a 7.0 mm optic and plate haptic design. J Cataract Refract Surg 2022;48:75–82
12. Makhotkina NY, Berendschot TT, Nuijts RM. Objective evaluation of negative dysphotopsia with Goldmann kinetic perimetry. J Cataract Refract Surg 2016;42:1626–1633
13. Holladay JT, Simpson MJ. Negative dysphotopsia: causes and rationale for prevention and treatment. J Cataract Refract Surg 2017;43:263–275
14. Simpson MJ. Mini-review: far peripheral vision. Vision Res 2017;140:96–105
15. Simpson MJ. Double image in far peripheral vision of pseudophakic eye as source of negative dysphotopsia. J Opt Soc Am A Opt Image Sci Vis 2014;31:2642–2649
16. Simpson MJ. Simulated images of intraocular lens negative dysphotopsia and visual phenomena. J Opt Soc Am A Opt Image Sci Vis 2019;36:B44–B51
17. Erie JC, Simpson MJ, Mahr MA. Effect of a 7.0 mm intraocular lens optic on peripheral retinal illumination with implications for negative dysphotopsia. J Cataract Refract Surg 2022;48:95–99
18. van Vught L, Dekker CE, Stoel BC, Luyten GPM, Beenakker JM. Evaluation of intraocular lens position and retinal shape in negative dysphotopsia using high-resolution magnetic resonance imaging. J Cataract Refract Surg 2021;47:1032–1038
19. Escudero-Sanz I, Navarro R. Off-axis aberrations of a wide-angle schematic eye model. J Opt Soc Am A Opt Image Sci Vis 1999;16:1881–1891

20. van Vught L, Beenakker JM. ZOSPy. v.0.5.1. 2021
21. Invernizzi A, Cigada M, Savoldi L, Cavuto S, Fontana L, Cimino L. In vivo analysis of the iris thickness by spectral domain optical coherence tomography. Br J Ophthalmol 2014;98:1245–1249
22. Simpson MJ. Intraocular lens far peripheral vision: image detail and negative dysphotopsia. J Cataract Refract Surg 2020;46:451–458
23. Das KK, Werner L, Collins S, Hong X. In vitro and schematic model eye assessment of glare or positive dysphotopsia-type photic phenomena: comparison of a new material IOL to other monofocal IOLs. J Cataract Refract Surg 2019;45:219–227
24. Johnson & Johnson Vision. TECNIS® monofocal 1-piece IOL. https://www.jnjvisionpro.com/products/tecnis%C2%AE-1-piece-iol. Accessed March 8, 2022
25. Nanavaty MA, Spalton DJ, Boyce J, Brain A, Marshall J. Edge profile of commercially available square-edged intraocular lenses. J Cataract Refract Surg 2008;34:677–686
26. Nanavaty MA, Zukaite I, Salvage J. Edge profile of commercially available square-edged intraocular lenses: Part 2. J Cataract Refract Surg 2019;45:847–853
27. Bausch & Lomb Incorporated. enVista IOL. https://www.bausch.com/ecp/our-products/cataract-surgery/lens-systems/envista-iol. Accessed March 8, 2022
28. Franchini A, Gallarati BZ, Vaccari E. Analysis of stray-light effects related to intraocular lens edge design. J Cataract Refract Surg 2004;30:1531–1536
29. van Vught L, Shamonin DP, Luyten GPM, Stoel BC, Beenakker JM. MRI-based 3D retinal shape determination. BMJ Open Ophthalmol 2021;6:e000855
30. Canovas C, Abenza S, Alcon E, Villegas EA, Marin JM, Artal P. Effect of corneal aberrations on intraocular lens power calculations. J Cataract Refract Surg 2012;38:1325–1332
31. Canovas C, Artal P. Customized eye models for determining optimized intraocular lenses power. Biomed Opt Express 2011;2:1649–1662
32. Tabernero J, Piers P, Benito A, Redondo M, Artal P. Predicting the optical performance of eyes implanted with IOLs to correct spherical aberration. Invest Ophthalmol Vis Sci 2006;47:4651–4658
33. Song H, Chui TY, Zhong Z, Elsner AE, Burns SA. Variation of cone photoreceptor packing density with retinal eccentricity and age. Invest Ophthalmol Vis Sci 2011;52:7376–7384
34. Rozendal L, van Vught L, Beenakker J, Luyten G. Clinical outcomes of bag-to-bag intraocular lens exchange with a wide optic lens for the treatment of dysphotopsia (Conference abstract). Acta Ophthalmol 2021;2021:43
35. Atchison DA, Pritchard N, Schmid KL, Scott DH, Jones CE, Pope JM. Shape of the retinal surface in emmetropia and myopia. Invest Ophthalmol Vis Sci 2005;46:2698–2707
36. Makhotkina NY, Dugrain V, Purchase D, Berendschot T, Nuijts R. Effect of supplementary implantation of a sulcus-fixated intraocular lens in patients with negative dysphotopsia. J Cataract Refract Surg 2018;44:209–218

Disclosures: *None of the authors has any financial or proprietary interest in any material or method mentioned.*

First author:
Luc van Vught, BSc

Department of Ophthalmology, Leiden University Medical Center, Leiden, the Netherlands